Electronic supplementary information for the following manuscript:

A highly selective fluorescence turn-on detection of ClO^- with 1-methyl-1,2-dihydropyridine-2-thione unit modified tetraphenylethylene

Xiaobiao Dong,[a b] Guanxin Zhang,*[a] Jinbiao Shi,[a b], Yuancheng Wang,[a b] Ming Wang,[a] Qian Peng, [a] Deqing Zhang*[a b]

[a]*CAS Key Laboratories of Organic Solids and Analytical Chemistry for Living Biosystems, CAS Research/Education Center for Excellence in Molecular Sciences, Institute of Chemistry, Chinese Academy of Sciences, Beijing 100190, P.R. China.*

[b] *University of Chinese Academy of Sciences, Beijing 100049, P. R. China*

Table of Contents

1. General information for synthesis and characterization

Instruments. ^{1}H NMR and ^{13}C NMR spectra were recorded on Bruker Avance 300 MHz. The HR-EI spectra and HR- ESI were recorded with Waters GCT and Bruker Solarix respectively. Fluorescence spectra were measured with a Jasco FP-6000 spectrometer. UV/Vis absorption spectra were recorded on Jasco V-570 spectrophotometer. Dynamic light scattering (DLS) experiments were carried out with Malvern Instrument (Nano Series). Confocal fluorescence imaging experiments were performed with an Olympus FV-1000 laser scanning microscopy system, based on an IX81 (Olympus, Japan) inverted microscope. The fluorescence quantum yields were measured by using HAMAMATSU Absolute PL Quantum Yield Spectrometer C11347 at the excitation wavelength of 380 nm for **1** and 400 nm for **1-ClO**. The pH meter was used to adjust the pH of the PBS solution. The MTT was measured by Btotek Synergy 1H'.

The single crystals of compound **2** and **1-ClO** were prepared by slow evaporation of dichloromethane and methanol respectively. All single crystals data were collected on Rigaku Saturn diffractometer with CCD area detector. All calculations were performed using the SHELXL97 and crystal structure crystallographic software packages. Crystallographic data (excluding structure factors) for the structures reported in this paper have been deposited with the Cambridge Crystallographic Data Centre as supplementary publication no. CCDC: 1533716 for compound **2**, 1533709 for **1-ClO**.

Materials. All reagents and solvents were obtained from commercial suppliers (Alfa Aesar, Acros, J&K) without further purification, but toluene was dried with sodium and distilled before used. 3-(4, 5-Dimethylthiazol-2-yl)-2, 5-diphenyltetrazolium bromide (MTT) and Hela cells were obtained from Sigma-Aldrich.

The hypochlorite(ClO^-), *tert*-butylhydroperoxide (*t*-BuOO•), superoxide (O_2^-), nitrite (NO_2^-), nitrate (NO_3^-), sulfate (SO_4^{2-}), sulfide (S^{2-}), acetate (AcO^-)，SO_3^{2-} and Cl^- were prepared from NaClO, *t*-BuOOH, KO_2, $NaNO_2$, $NaNO_3$, Na_2SO_4, Na_2S, AcOK, Na_2SO_3 and NaCl respectively. The hydroxyl radical (•OH) was prepared by Fenton reactions, and the single oxygens ($^1O_2$) was generated from 3,3'-(naphthalene-

1,4-diyl)dipropionic acid.[S1] The peroxynitrite ($ONOO^-$) solution was synthesized as reported.[S1] Nitric oxide (NO) was generated from sodium nitroferricyanide (III) dihydrate (SNP).[S1] Hydrogen peroxide (H_2O_2), sodium hypochlorous (NaClO), *t*-BuOOH, KO_2, $NaNO_2$, $NaNO_3$, Na_2SO_4, Na_2S, AcOK， Na_2SO_3，NaCl, 3,3'-(naphthalene-1,4-diyl)dipropionic acid and SNP was commercial available. Before use, hydrogen peroxide was diluted immediately from a stabilized 30% solution, and was assayed by using 43.6 $M^{-1}cm^{-1}$ as the molar absorptivity at 240 nm[S2], and sodium hypochlorous was assayed using a molar absorptivity of 391 $M^{-1}cm^{-1}$ at 292 nm. [S2] The hypobromite was generated from the reaction 1.0 g NaOH with 1.0 g brown-red solution of Br_2 in the iced water, The lambert-Beer's law was used to calculate the concentration of BrO^- (ε_{329} = 332 L mol^{-1} cm^{-1}).[S3] Compound **5** was synthesized according to previous report.[S4]

ClO^- detection in living cells. HeLa cells (ATCC, Manassas, VA) were maintained in high glucose DMEM (Dulbecco's Modified Eagle's medium, HyClone, UT) supplemented with 10% FBS (fetal bovine serum, HyClone, UT) and 1% penicillin-streptomycin (GIBCO, CA). To conduct the fluorescent imaging of ClO^-, HeLa cells were first seeded on glass-bottom culture dishes (Nest, China) for 24 h at a density of 1×10^5 cells/mL. At the day of experiment, the cells were treated with 0, 20, 60, 100 μM of NaClO for 30 min., and thoroughly wished with PBS before adding 10 μM of probe **1**. The cells were incubated with the compound **1** for 2 h, and washed with PBS for two times before CLSM imaging.

Cytotoxicity Assay of compound 1. To study the biocompatibility of compound **1** in living cells, HeLa cells were seeded in a 96-well plate at a density of 1×10^4 per well and incubated with probe **1** with concentrations ranging from 20 to 2.5 μM for 2h. The mixed medium were replaced with fresh cell culture medium, followed by additional 48 h of incubation. The cell viability was measured MTT assay according to a standard protocol.[S5]

2. Synthesis

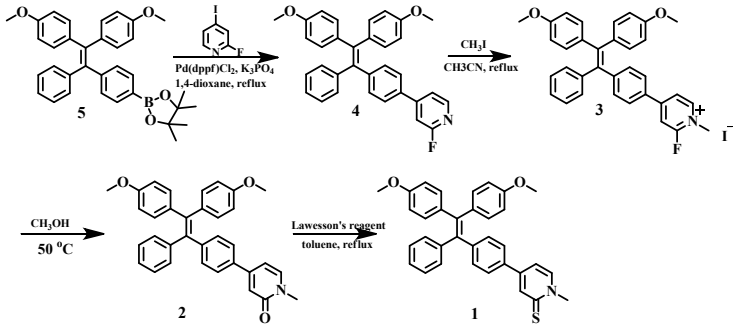

Scheme S1 Synthetic approach to compound **1**

Synthesis of compound 4. A mixture of compound **5** (1036.9 mg, 2.0 mmol), 2-fluoro-4-iodopyridine (668.9 mg, 3.0 mmol), $Pd(PPh_3)_4$ (115.6 mg, 0.1 mmol), K_2CO_3 (2mL, 2M) in THF (30 mL) were refluxed overnight under nitrogen. After cooling to room temperature, the solvent was evaporated under reduced pressure. The residue was dissolved in CH_2Cl_2 and the organic phase was washed with water for three times. The organic layer was dried with anhydrous Na_2SO_4, filtered and evaporated. The residue was subjected to column chromatography with CH_2Cl_2/PE (v/v, 3/1) as eluent. Compound **4** was obtained as yellow solid (731.4 mg, 1.5 mmol) in 75.0% yield. ^{1}H NMR (300 MHz, $CDCl_3$): δ 8.21 (1H, d, *J* =5.1 Hz), 7.41-7.35 (3H, m), 7.15-7.03 (8H, m), 6.99-6.93 (4H, m), 6.68-6.63 (4H, m), 3.75 (6H, s). ^{13}C NMR (75 MHz, $CDCl_3$): δ 166.16, 163.01, 158.37, 158.27, 153.66, 153.55, 147.98, 147.77, 146.23, 143.90, 141.29, 138.12, 136.00, 134.19, 134.14, 132.64, 132.60, 132.24, 131.41, 127.88, 126.38, 126.26, 119.16, 119.11, 113.21, 113.05, 106.86, 106.36, 55.13, 55.12. HR-EI: calcd. for $C_{33}H_{26}NO_2F$: 487.1948; Found: 487.1950.

Synthesis of compound 2. A mixture of compound **4** (487.6 mg, 1.0 mmol) and iodomethane (425.8 mg, 3 mmol) in CH_3CN (20 mL) were heated in 50 °C overnight. After cooling to room temperature, the solvent was evaporated under reduced pressure. The residue was dissolved in CH_3OH and heated in 50 °C for 30 minutes. Then the solvent was evaporated under reduced pressure and subjected to column chromatography with CH_2Cl_2/CH_3OH (v/v, 50/1) as eluent. Compound **2** was obtained as yellow solid (479.6 mg, 0.96 mmol) in 96.0% yield. ^{1}H NMR (300 MHz, $CDCl_3$): δ 7.31-7.26 (3H, m), 7.13-7.02 (7H, m), 6.97-6.92 (4H, m), 6.77 (1H, d, *J*=

1.2 Hz), 6.67-6.62 (4H, m), 6.40 (1H, dd, J_1= 1.8 Hz, J_2=6.9 Hz), 3.75 (3H, s), 3.74 (3H, s), 3.56 (3H, s). ^{13}C NMR (75MHz, $CDCl_3$): δ 163.30, 158.32, 158.20, 151.36, 145.88, 143.96, 141.09, 138.28, 137.92, 136.08, 136.04, 134.55, 132.63, 132.60, 131.99, 131.41, 127.84, 126.31, 125.97, 116.39, 113.18, 113.02, 105.31, 55.13, 55.10, 37.31. HR-EI: calcd. for $C_{34}H_{29}NO_3$: 499.214726; Found: 499.214733.

Synthesis of compound 1. A mixture of compound **2** (249.8 mg, 0.5 mmol) and Lawesson's reagent (121.3 mg, 0.3 mmol) in anhydrous toluene (10 mL) were refluxed for 1h under nitrogen. After cooling to room temperature, the solvent was evaporated under reduced pressure. The residue subjected to column chromatography with CH_2Cl_2 as eluent. Compound **1** was obtained as orange solid (232.5 mg, 0.45mmol) in 90.0% yield. ^{1}H NMR (300 MHz, DMSO-d_6): δ 8.19 (1H, d, *J*=9.0 Hz), 7.71 (1H, d, *J*=3.0 Hz), 7.61 (2H, d, *J*=9.0 Hz), 7.18-7.09 (4H, m), 7.06 (2H, d, *J*=9.0 Hz), 6.99-6.96 (2H, m), 6.92-6.85 (4H, m), 6.73-6.67 (4H, m), 3.85 (3H, s), 3.67 (6H, s). ^{13}C NMR (75 MHz, DMSO-d_6): δ 179.06, 158.46, 158.32, 146.25, 144.81, 144.03, 143.19, 141.30, 138.36, 135.95, 135.83, 133.21, 132.56, 132.52, 132.06, 131.29, 130.01, 128.47, 126.82, 113.85, 113.66, 111.43, 55.41, 45.03. HR-EI: calcd. for $C_{34}H_{29}NO_2S$: 515.1919; Found: 515.1916.

Synthesis of compound 1-ClO. NaClO (30 mL, 1mM) was added slowly to the solution of compound **1** (51.6 mg, 0.1 mmol) in CH_3CN under stirring. Then the solution was poured into water (100 mL) andextracted by CH_2Cl_2, The organic layer was dried with anhydrous Na_2SO_4, filtered and evaporated. The residue was subjected to column chromatography with CH_2Cl_2/CH_3OH (v/v, 20/1) as eluent. Compound **1-ClO** was obtained as red solid (39.4 mg, 0.07 mmol) in 70.0% yield. ^{1}H NMR (300 MHz, DMSO-d_6): δ 8.97 (1H, d, *J*=6.6Hz), 8.51 (1H, d, *J*=2.4Hz), 8.39(1H, dd, J_1= 2.4 Hz, J_2=6.6 Hz), 7.86(2H, d, *J*=8.4Hz), 7.20-7.13 (5H, m), 7.02-6.99 (2H, m), 6.94-6.87 (4H, m), 6.75-6.69 (4H, m), 4.52 (3H, s), 3.682 (3H, s), 3.677 (3H, s). ^{13}C NMR (75 MHz, DMSO-d_6): δ 158.65, 158.46, 157.50, 155.50, 148.79, 143.76, 142.19, 137.99, 135.61, 132.65, 132.57, 131.33, 131.27, 128.56, 128.08, 124.02, 122.25, 113.93, 113.69, 55.44, 46.25. HR-ESI: calcd. for $C_{34}H_{29}NO_5SNa^+$(M+Na^+): 586.1659; Found: 586.1656.

3. Comparison with lately reported fluorescent probes for ClO^-

Table S1 Comparison of lately reported fluorescent probes for ClO^-

Reference	Structure	Reaction time	The limit of detection	Solvent
Chem. Commun., 2016[8b]	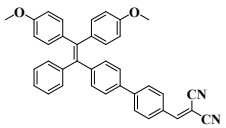	180 s	470 nM	PBS buffers (pH=7.4, 1% DMSO and 1mM CTAB)
Chem. Commun., 2017[7d]	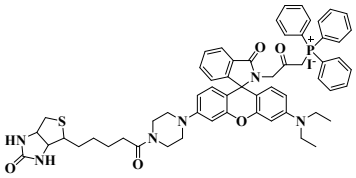	A few seconds	210 nM	PBS buffers (pH=7.4, 20% EtOH)
ACS Appl. Mater. Interfaces, 2016[7e]	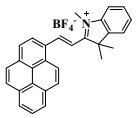	70 minutes	350 nM	PBS buffers (pH=7.4, 5% DMSO)
J. Mater. Chem. B, 2017[9c]	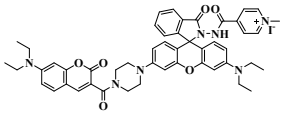	60 s	70 nM	PBS buffers (pH=7.4, 0.5% EtOH)
Chem. Commun., 2013[9d]	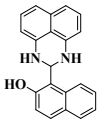	1 minute	56 nM	CH_3CN : H_2O (6 : 4, v/v)
Chem. Commun., 2015[10d]	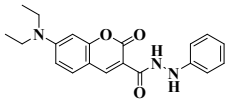	5 minutes	356 nM	PBS buffers (pH=7.4, 20% CH_3CN)
Anal. Chem., 2016[13a]	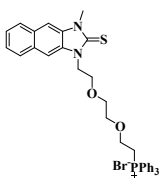	<3 minutes	210 nM	PBS buffers (pH=7.4, 0.2% DMF)
This work	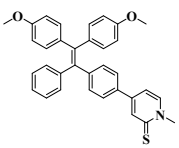	<40 s	92 nM	PBS buffers (pH=7.4, 0.5% DMSO)

We have compared the probe **1** with the reported probes for ClO^-, and the results are listed in Table S1. In comparison with the reported probes, probe **1** has the following advantages: i) the response time is short, ii) the sensitivity is relatively high and iii) the detection can be carried out in almost aqueous solution. Though the probes repored in ref. 9c and 9d have almost similar sensitivity and response time towards ClO^-, drawbacks still exist for both probes. For instance, the probe in ref. 9c was synthesized in multi-steps, while acetonitrile as co-solvent was used for the detection of ClO^- with the probe in ref. 9d.

4. Crystal structures and crystallographic data for 2 and 1-ClO

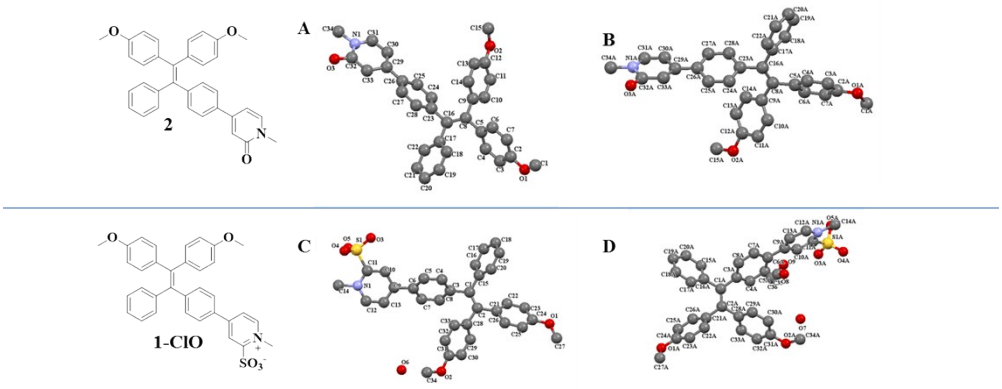

Fig. S1 The crystal structures of compound **2** (up) and **1-ClO** (down): Two conformations were found within the crystal of **2** (A and B) and **1-ClO**(C and D), respectively.

Table S2. Crystallographic data for **2** and **1-ClO**

	2	**1-ClO**
Formula	$C_{34}H_{29}NO_3$	$C_{35}H_{34.4}NO_{6.7}S$
fw	**499.58**	**563.18**
Crystal system	**Triclinic**	**Monoclinic**
space group	**P -1**	**P 1 21/c 1**
a(Å)	**9.806(2)**	**10.795(2)**
b(Å)	**10.498(2)**	**9.810(2)**
c(Å)	**25.685(5)**	**58.340(13)**
α (deg)	**88.718(6)**	**90**

β (deg)	**87.656(6)**	**90.622**
γ (deg)	**89.387(6)**	**90**
V (Å^3)	**2641.2(10)**	**6178(2)**
Z	**4**	**8**
Dcalcd. (Mg/cm^3)	**1.256**	**1.307**
θ range (^{o})	**1.587 to 27.477**	**1.887 to 27.467**
F (000)	**1056**	**2566**
R (int)	**0.0552**	**0.0408**
GOF on F^2	**1.155**	**1.126**
R_1 [I>2σ(I)]	**0.0875**	**0.0702**
wR_2	**0.1958**	**0.1502**
CCDC no.	**1533716**	**1533709**

5. Theoretical calculations of HOMO/LUMO levels

The fluorescence quenching for **1** is attributed to the photo-induced electron transfer (PET) from TPE core to the 1-methyl-1,2-dihydropyridine-2-thione moiety. In order to support this assumption, HOMO/LUMO levels of the electron donor and acceptor moieties were calculated. **1-TPE** and **1-S** (shown in Fig. S2) were used as models for the respective electron donor and acceptor moieties of **1**. The theoretical calculations were performed with Gaussian 16 package. Geometries optimization and frequency analysis were performed at the level of B3LYP/6- 31G* (d, p). Tables S3 and S4 listed the coordinates and energies at the optimized geometries for **1-S** and **1-TPE**, and there were no any imaginary frequencies. Then, the molecular orbitals were analyzed.

As shown in Fig. S2, evidently, the HOMO and LUMO levels of **1-S** are lower than those of **1-TPE**. Thus, when **1-TPE** unit within compound **1** is excited, the electron in a ground state orbital is promoted to its lowest unoccupied molecular orbital (LUMO), which further transfers to the LUMO of **1-S**. This PET reaction is thermodynamically favorable on the basis of the HOMO and LUMO levels of **1-S** and **1-TPE** as shown in

Figure S2. It is expected that the photoinduced electron transfer process competes favorably with radiative decay to the ground state. Thus, weak fluorescence of **1** can be attributed to the PET process from TPE unit to the 1-methyl-1,2-dihydropyridine-2-thione moiety within **1**.

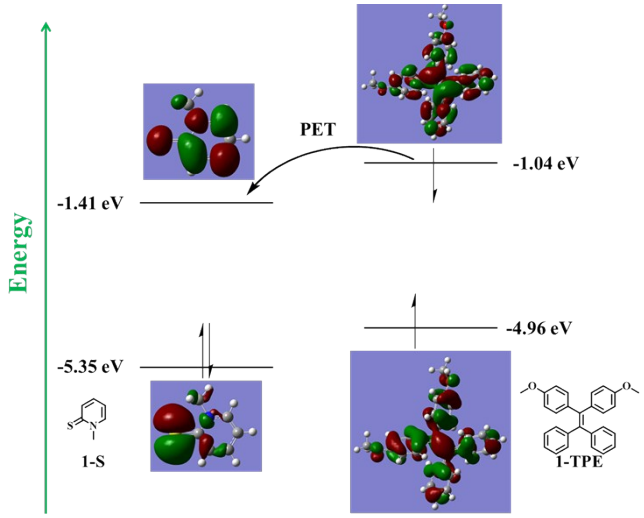

Fig. S2 The calculated HOMO and LUMO energy levels of **1-TPE** and **1-S**, corresponding to the electron donor and acceptor moieties of **1**.

Table S3. Coordinates and energy of **1-TPE**

		X	Y	Z
1	C	-3.5881823	-2.38108102	-0.38847553
2	C	-3.36024833	-1.29737983	-1.24939803
3	C	-2.21440864	-0.52779274	-1.11521955
4	C	-1.25248611	-0.80759503	-0.12484509
5	C	-1.48883147	-1.90942733	0.70974701
6	C	-2.64285711	-2.68649066	0.59732929
7	C	-0.00000659	-0.00453352	0.00053799
8	C	1.25219943	-0.80787656	0.12558759
9	C	0.00010406	1.36362872	0.00046913
10	C	1.2483865	2.17118763	-0.15807534
11	C	-1.24779666	2.17170287	0.15856856
12	C	1.51329617	3.25432908	0.69869591
13	C	2.66141635	4.02900882	0.5426127
14	C	3.56122896	3.75215013	-0.48832325
15	C	3.30117314	2.69354528	-1.36055126
16	C	2.15853874	1.91248891	-1.19727546
17	C	2.2153813	-0.52741555	1.11459581
18	C	3.36114428	-1.29719241	1.24822661
19	C	3.58780414	-2.38180046	0.38810951

20	C	2.6412259	-2.68794836	-0.59626843
21	C	1.4872989	-1.91066861	-0.70813146
22	C	-1.5110075	3.25602822	-0.6972774
23	C	-2.65893255	4.03112957	-0.54186454
24	C	-3.56031056	3.75356874	0.48751025
25	C	-3.30194806	2.69384833	1.35888592
26	C	-2.15952315	1.91237307	1.19626118
27	O	-4.74618398	-3.07376415	-0.59841606
28	C	-5.02705023	-4.18087153	0.24264855
29	O	4.74589879	-3.07453654	0.59736846
30	C	5.02534866	-4.18276889	-0.24270666
31	H	-4.09494959	-1.08287246	-2.01851648
32	H	-2.05323739	0.30614268	-1.7899723
33	H	-0.75744273	-2.16430207	1.47066561
34	H	-2.78885684	-3.52047985	1.2735097
35	H	0.81148439	3.48394842	1.4948521
36	H	2.85115388	4.85296702	1.22484297
37	H	4.45261878	4.35968728	-0.61502017
38	H	3.98769764	2.47719235	-2.17427408
39	H	1.96218409	1.09185134	-1.87930181
40	H	2.05520629	0.30712822	1.78882005
41	H	4.09673481	-1.08215028	2.01633986
42	H	2.78616629	-3.52270934	-1.27172017
43	H	0.75498595	-2.16608568	-1.46797343
44	H	-0.80802585	3.48623607	-1.49221678
45	H	-2.84727728	4.85593897	-1.22345083
46	H	-4.45155384	4.36142616	0.61370485
47	H	-3.98962013	2.47698158	2.17150442
48	H	-1.96451917	1.09098033	1.87775387
49	H	-5.98565589	-4.57918141	-0.09305908
50	H	-4.26139336	-4.96243295	0.15440405
51	H	-5.11048237	-3.88029337	1.29498223
52	H	5.98413842	-4.58108568	0.09244268
53	H	4.25941591	-4.96386386	-0.15269112
54	H	5.10776613	-3.88349932	-1.2954895

Total energy: -1231.88766514 Hartrees

Table S4. Coordinates and energy of **1-S**

		X	**Y**	**Z**
1	C	1.85585664	-1.24446802	-0.00001624
2	C	0.50743301	-1.48093262	0.00008938
3	C	-0.461934	-0.42432028	0.00004587
4	N	0.07599351	0.86797263	0.0000776

5	C	1.42467178	1.10268372	-0.00001069
6	C	2.33860775	0.0888513	-0.00007983
7	S	-2.1246423	-0.69620146	-0.00005041
8	C	-0.8443518	2.00933137	0.00002245
9	H	0.11087899	-2.48857778	0.00017144
10	H	1.71623961	2.14595613	-0.00001237
11	H	3.39717093	0.31666382	-0.00009121
12	H	-0.2616224	2.93113066	0.00133351
13	H	-1.4874954	1.9642433	-0.88131459
14	H	-1.4892584	1.96274305	0.87995224
15	H	2.55470793	-2.07561702	-0.00008138

Total energy: -685.80065365 Hartrees

6. The absorption spectra of the PBS solution of 1 before and after reaction with different amounts of ClO^-

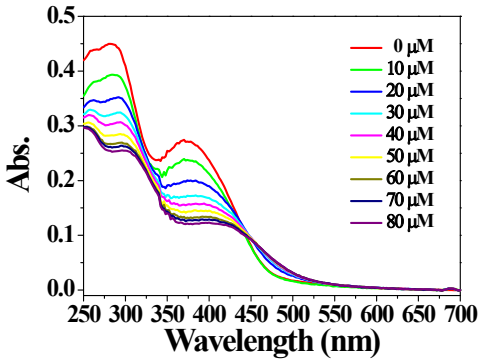

Fig. S3 The absorption spectra of the PBS solution (10 mM, pH= 7.4) of **1** (10.0 μM) in the presence of ClO^- (from 0 to 80.0 μM).

7. High-resolution mass spectrum of compound 1 after reaction with ClO^-

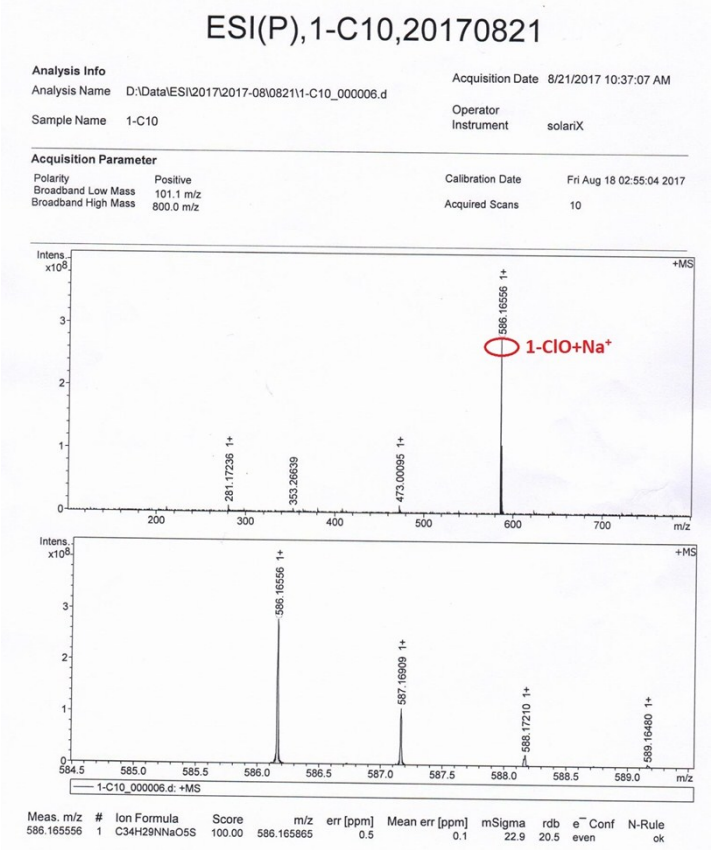

Fig. S4 High-resolution mass spectrum of compound **1** (100 μM) in PBS solution after reaction with ClO^- (1.0 mM).

8. DLS profiles of compound 1 before and after reaction with ClO^-.

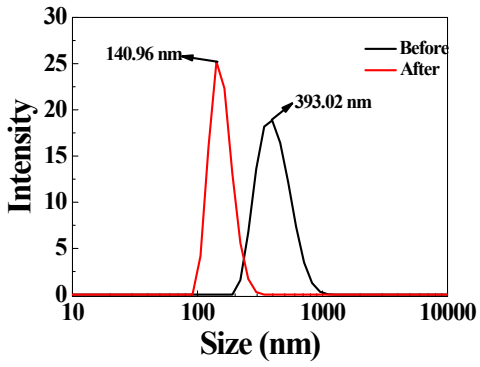

Fig. S5 DLS profiles of the PBS solution of compound **1** (10.0 μM) before (black) and after the reaction with ClO^- (70 μM, red).

9. SEM and TEM images of 1 before and after reaction with ClO^-

SEM images were taken with Hitachi S-4800 microscopy equipped with a digital

camera. The samples were prepared as follows: i) a carbon coated TEM grid was placed on a filter paper; ii) 100 μL solutions of **1** (10.0 μM) in PBS before and after addition of ClO^- (70.0 μM) were separately dropped onto the carbon coated TEM grids; the solvents were absorbed by the filter papers quickly. Thus, these procedures were expected to avoid the formation of aggregates due to evaporation of solvents during the sample preparation; iii) then, the samples were spluttered with platinum for SEM measurements. TEM images were taken with JEM-2100F microscopy. The TEM samples were prepared by the same procedure but without platinum sputtering before TEM measurements.

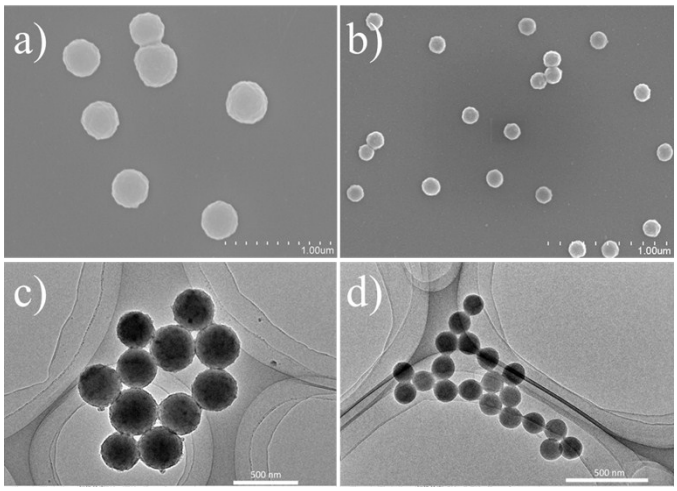

Fig.S6 SEM and TEM images of PBS solution of **1** (10 μM) before (SEM: a, TEM: c) and after (SEM: b, TEM: d) addition of ClO^- (70 μM).

10. AFM images of 1 before and after reaction with ClO^-

Atomic force microscopy (AFM) images of **1** before and after reaction with ClO^- were obtained on a Bruker Nanoscope V AFM (Digital instruments) operating in tapping mode. The AFM samples were prepared as follows: i) dropping 100 μL PBS solution of **1** (10 μM) before and after addition of ClO^- (70 μM) separately on the surface of silicon slice which was treated with plasma; ii) after evaporation of the solution at room temperature, the silicon slices were washed with deionized cold water for three times to remove inorganic salts. iii) Then these samples were dried under vacuum at room temperature for two hours before measurement.

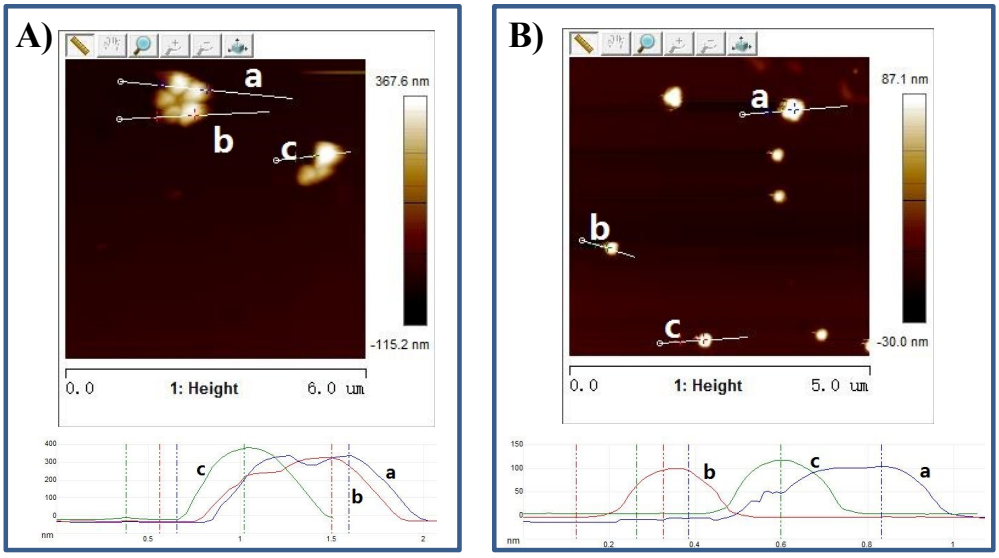

Fig. S7 AFM images of particles of **1** (10 μM in aqueous solution) before (A) and after (B) treatment with ClO^- (70 μM).

11. Fluorescence microscopy images of 1 before and after reaction with ClO^-

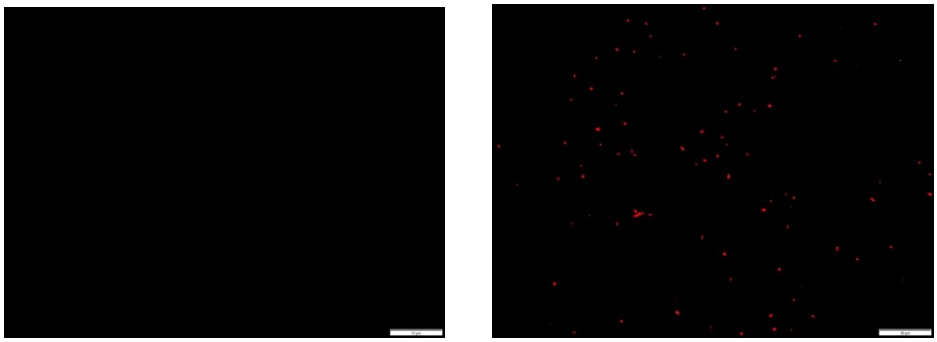

Fig. S8 Fluorescence microscopy images of compound **1** (10.0 μM) before (*left*) and after (*right*) addition of ClO^- (70.0 μM) with an excitation wavelength of 405 nm. The scale bar represents 10.0 μm.

12. Fluorescence spectra of 1-ClO in THF/H_2O mixtures with different volume fraction of H_2O

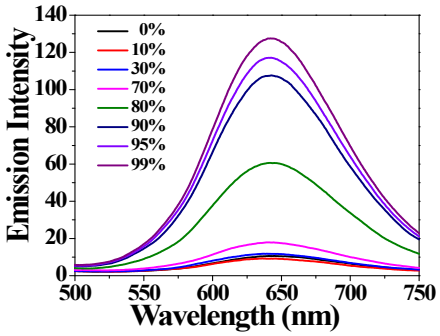

Fig. S9 Fluorescence spectra of **1-ClO** (10 μM) in THF/H_2O mixtures with different volume fraction of H_2O (0-99%).

13. The effect of pH on the reaction of compound 1 with ClO^-

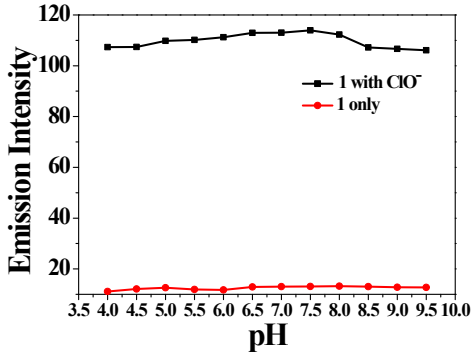

Fig. S10 The variation of the fluorescence intensity at 620 nm of the PBS solution (10 mM) of **1** (10 μM) at different pH values (from 4.0 to 9.5) in the absence (red) and presence (black) of ClO^- (70 μM).

14. Estimation of the detection limit

The detection limit was calculated according to the equation (1):

The detection limit = $3\sigma / k$ (1)

Where σ = standard deviation of 11 blank solution and k = the slope of the graph of the fluorescence intensity at 620 nm and the concentration of ClO^- (Fig. 1c). The detection of limit was found to be 92 nM.

15. Photos of the filter papers containing spots of 1 under UV light upon addition of ClO^- and other species

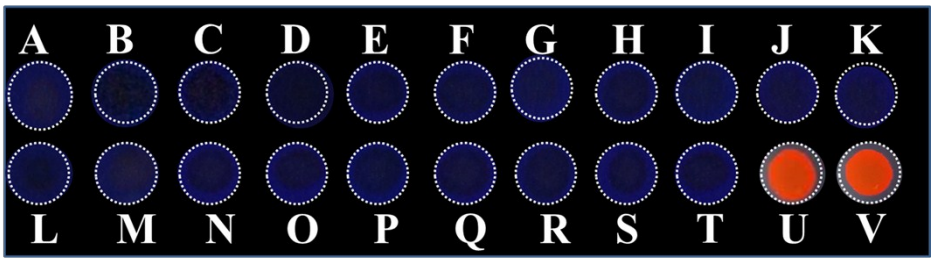

Fig. S11 The photos of the filter papers containing spots of **1** (30 μM, 2 μL) under UV light (365 nm) before (upper) and after (bottom) addition of other species and ClO^-: A (I^-), B(Br^-), C(Cl^-), D (F^-), E (SO_3^{2-}), F (S^{2-}), G (SCN^-) ,H (N_3^-), I (NO_2^-), J (Ag^+), K (Mg^{2-}), L (Fe^{2+}), M (Zn^{2+}), N (Hg^{2+}), O (Fe^{3+}), P (t-BuOO$^\bullet$), Q (H_2O_2), R ($ONOO^-$), S ($^\bullet OH$), T (blank), U (BrO^-) and V (ClO^-), respectively. The concentration of ClO^- and BrO^- was 100 μM in water, while the concentration of each other species was 1.0 mM and 2 μL of each species solution was used for the experiments.

16. Cytotoxicity of compound 1 toward Hela cells

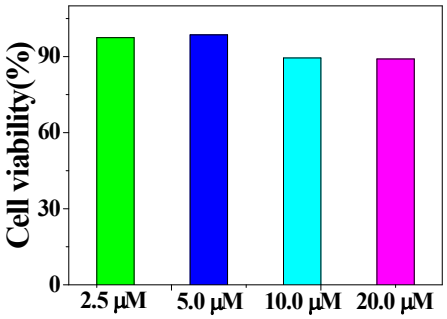

Fig. S12 Cytotoxicity of compound **1** toward Hela cells; Hela cells were incubated with compound **1** of different concentrations (2.5, 5, 10, 20 μM) for 12 hours, followed by a standard MTT assay.

17. Photostability of compound 1 for fluorescence imaging of HeLa cells after treatment with ClO^-

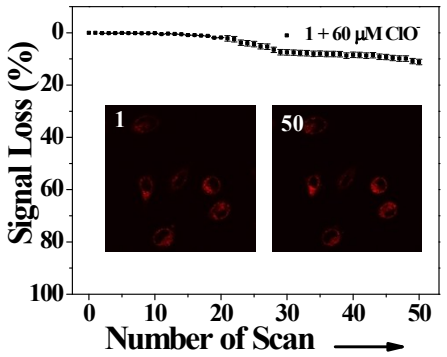

Fig. S13 Photostability of **1** in ClO^- (60 μM) stained HeLa cells: signal loss of fluorescence intensity of **1** after continuously scanning; inset shows CLSM images of stained HeLa cells after one and 50 scans, respectively. The photostability was evaluated by scanning the stained Hela cells for continuous 50 times using λ_{ex} = 405 nm lasers (scanning frequency = 5 s); the red channel was set at 600 ± 50 nm.

18. ^{1}H NMR and ^{13}C NMR spectra of 1-4 and 1-ClO

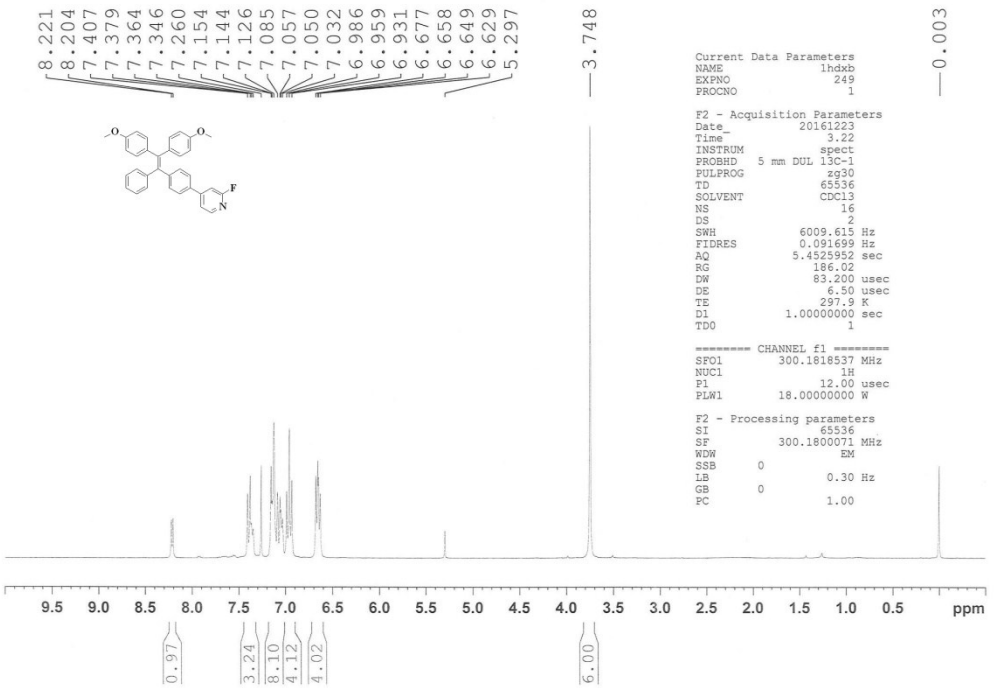

Fig. S14. ^{1}H NMR spectrum of compound **4** in $CDCl_3$.

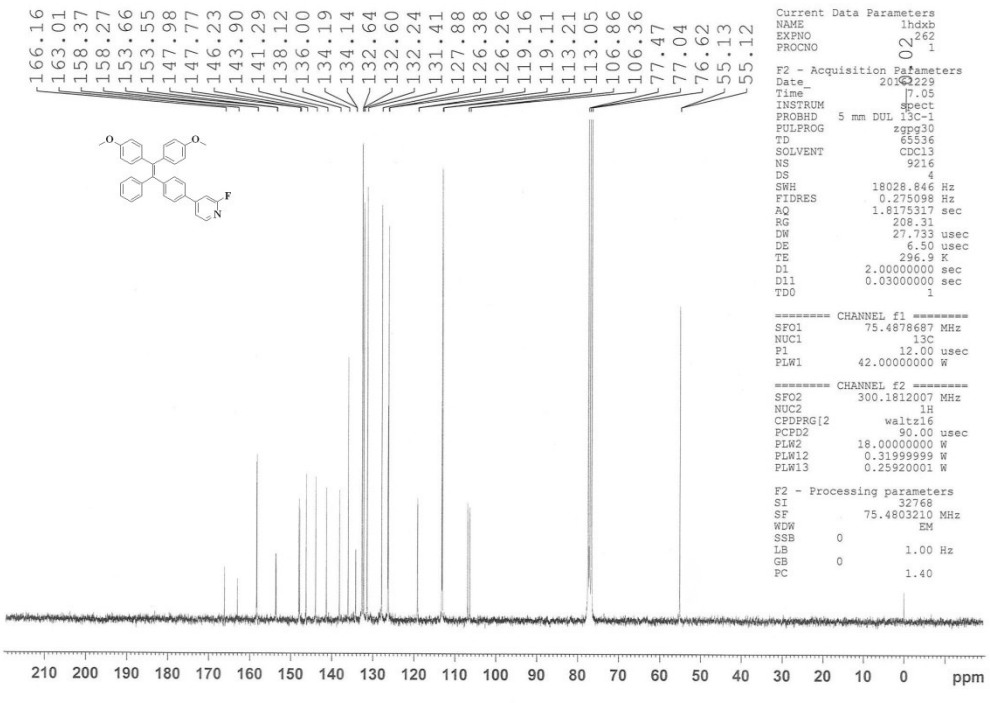

Fig. S15. ^{13}C NMR spectrum of compound **4** in $CDCl_3$.

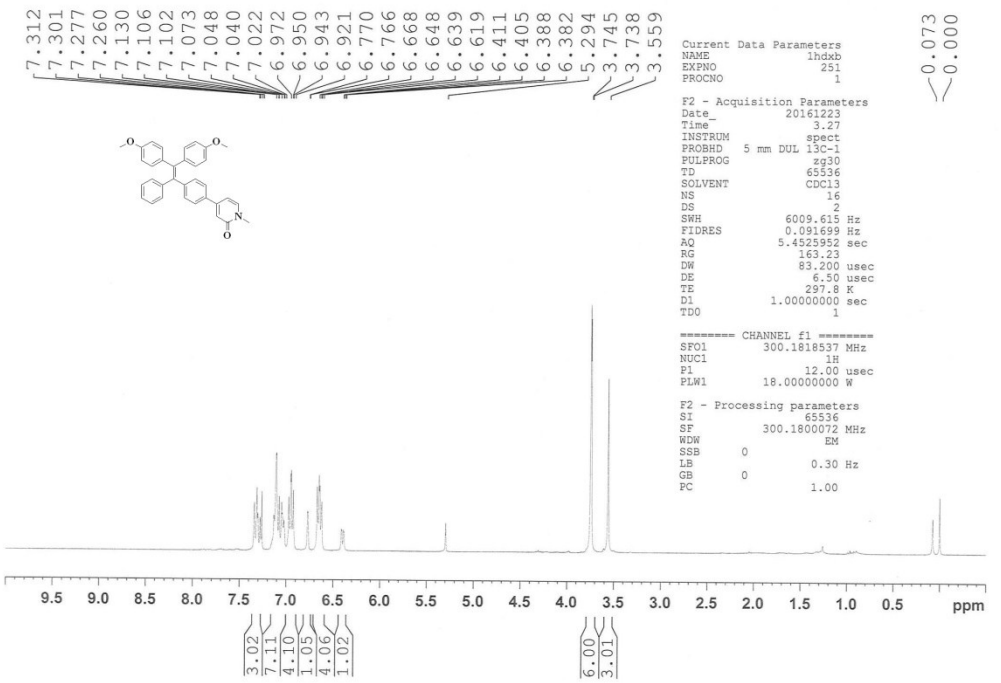

Fig. S16. ^{1}H NMR spectrum of compound **2** in DMSO**.**

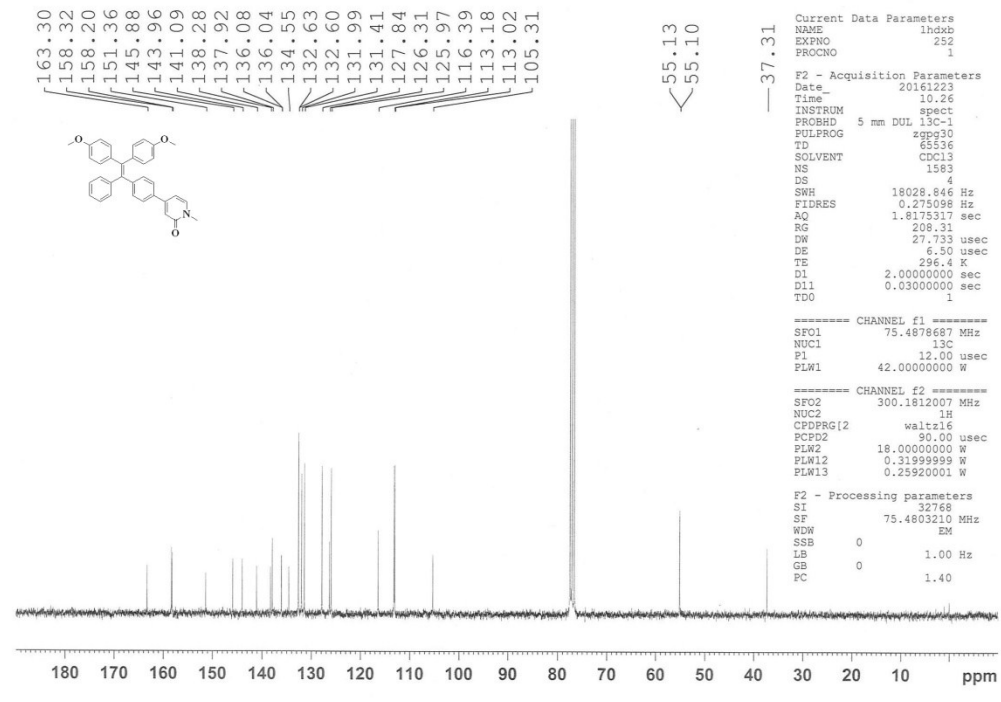

Fig. S17. ^{13}C NMR spectrum of compound **2** in DMSO**.**

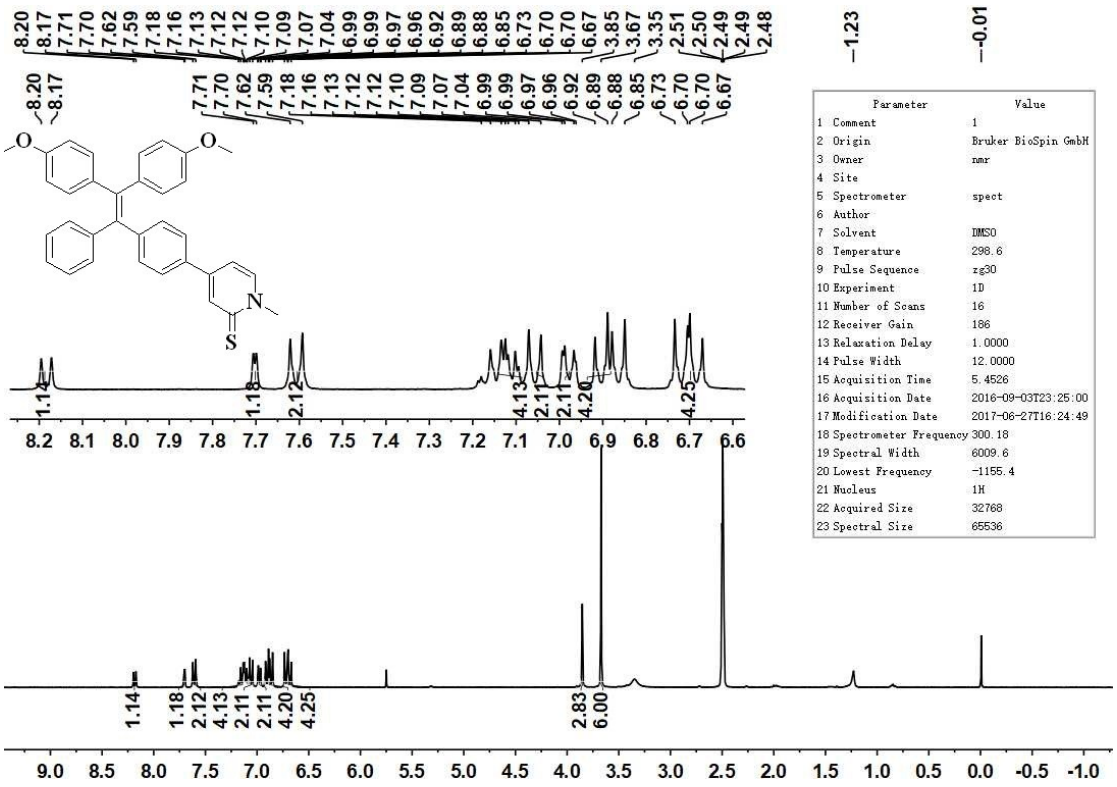

Fig. S18. ^{1}H NMR spectrum of compound **1** in DMSO**.**

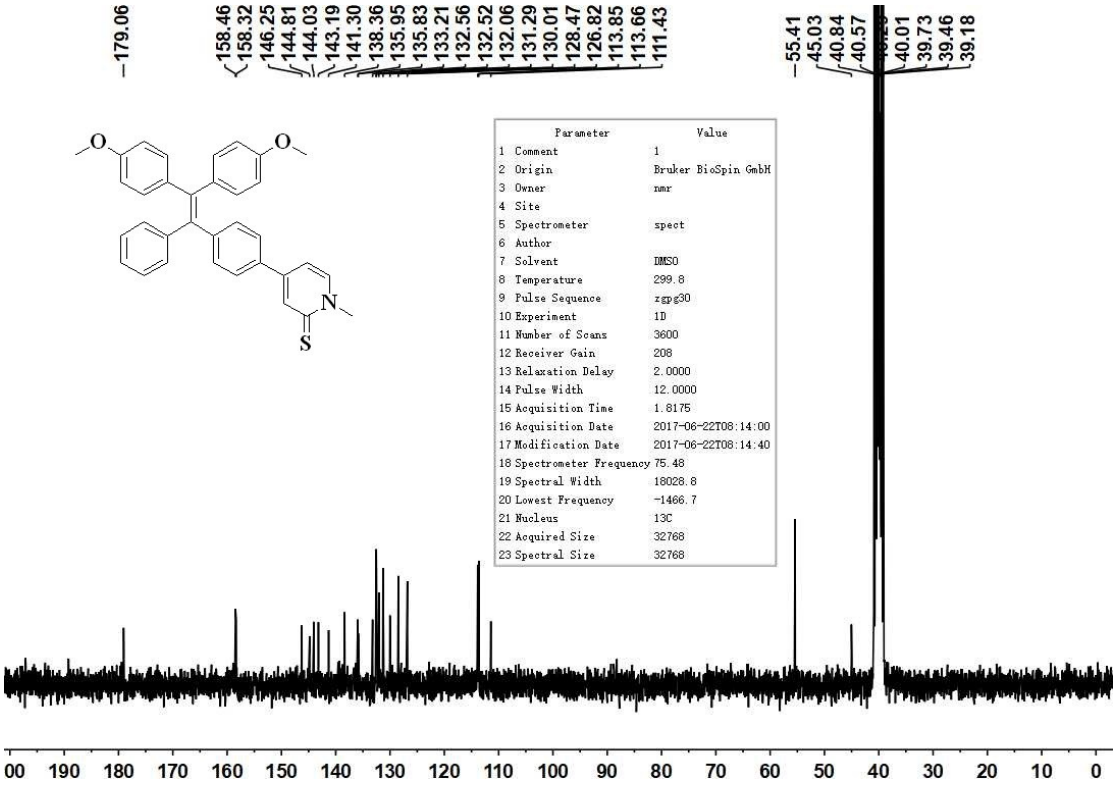

Fig. S19. ^{13}C NMR spectrum of compound **1** in DMSO**.**

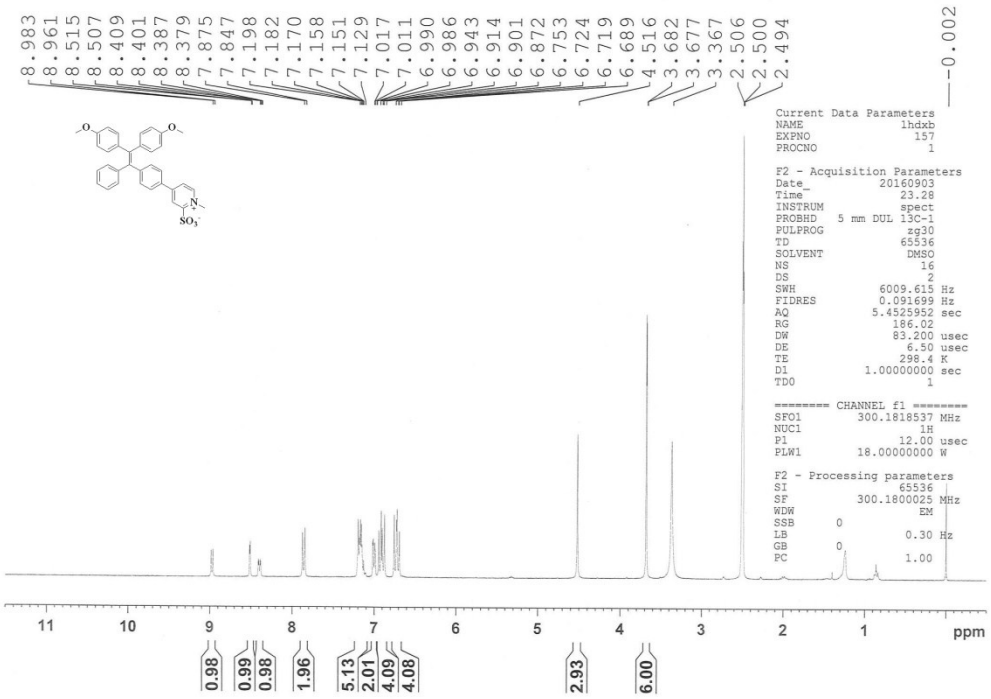

Fig. S20. ^{1}H NMR spectrum of compound **1-ClO** in DMSO**.**

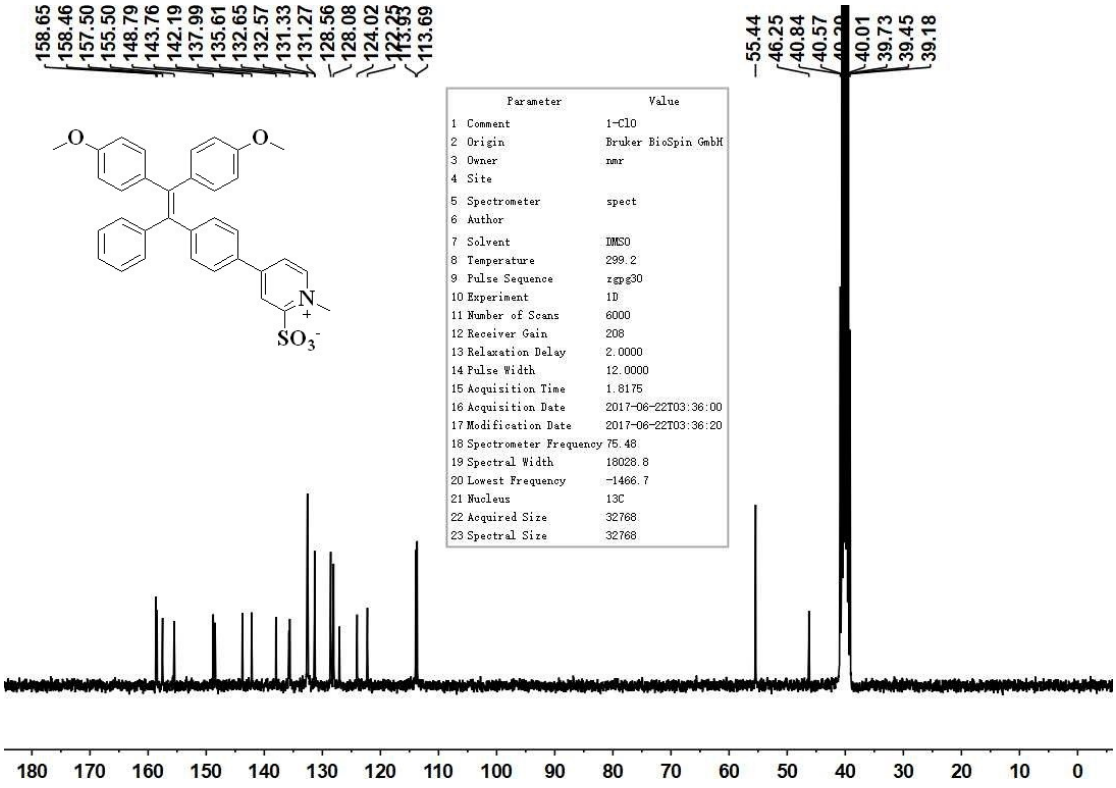

Fig. S21. ^{13}C NMR spectrum of compound **1-ClO** in DMSO**.**

References:

S1. Z. N. Sun, F. Q. Liu, Y. Chen, P. K. H. Tam and D. Yang, *Org. Lett.*, 2008, **10**, 2171.

S2. X. H. Li, G. X. Zhang, H. M. Ma, D. Q. Zhang, J. Li and D. B. Zhu, *J. Am. Chem. Soc.*, 2004, **126**, 11543.

S3. K. H. Xu, D. R. Luan, X. T. Wang, B. Hu, X. J. Liu, F. P. Kong and B. Tang, *Angew. Chem. Int. Ed.*, 2016, **55**, 12751

S4. Y. Y. Yuan, S. D. Xu, X. M. Cheng, X. L. Cai and B. Liu, *Angew. Chem. Int. Ed.*, 2016, **55**, 6457.

S5. (a) Y. Huang, P. S. Zhang, M. Gao, F. Zeng, A. J. Qin, S. Z. Wu and B. Z. Tang, *Chem. Commun.*, 2016, **52**, 7288; (b) B. P. Guo, H. L. Nie, W. Yang, Y. Tian, J. Jing, X. L. Zhang, *Sens. Actuators B Chem.*, 2016, **236**, 459.